Entraining the topology and the dynamics of a network of phase oscillators

I. Sendiña-Nadal,[1] I. Leyva,[1] J. M. Buldú,[1] J. A. Almendral,[1] and S. Boccaletti[2,3]

[1]*Complex Systems Group, Universidad Rey Juan Carlos, c/Tulipán s/n, 28933 Móstoles, Madrid, Spain*
[2]*Embassy of Italy in Tel Aviv, 25 Hamered Street, 68125 Tel Aviv, Israel*
[3]*CNR-Istituto dei Sistemi Complessi, Via Madonna del Piano, 10, 50019 Sesto Fiorentino (Fi), Italy*

We show that the topology and dynamics of a network of unsynchronized Kuramoto oscillators can be simultaneously controlled by means of a forcing mechanism which yields a phase locking of the oscillators to that of an external pacemaker in connection with the reshaping of the network's degree distribution. The entrainment mechanism is based on the addition, at regular time intervals, of unidirectional links from oscillators that follow the dynamics of a pacemaker to oscillators in the pristine graph whose phases hold a prescribed phase relationship. Such a dynamically based rule in the attachment process leads to the emergence of a power-law shape in the final degree distribution of the graph whenever the network is entrained to the dynamics of the pacemaker. We show that the arousal of a scale-free distribution in connection with the success of the entrainment process is a robust feature, characterizing different networks' initial configurations and parameters.

I. INTRODUCTION

The last decade has seen an increasing interest from the scientific community toward the study of complex networks, i.e., ensembles of interacting nodes whose connectivity structure is irregular, complex, and possibly evolving in time, with the main focus moving from the analysis of small networks to that of systems with thousands or millions of nodes, and with a renewed attention to the properties of networks of dynamical units [1,2].

A series of unifying principles and statistical properties common to most of the real networks has been unraveled. Probably, the most important of them is the scaling of the degree distribution of real world networks. The degree distribution $P(k)$ (defined as the probability that a node chosen uniformly at random has degree k) has been found to ubiquitously and significantly deviate from the Poisson or Gaussian distributions expected from random graphs and, in many cases, to exhibit a power-law [scale-free (SF)] tail [i.e., $P(k) \sim k^{-\gamma}$] with an exponent γ taking a value between two and three.

Consequently, most of the early attention of the scientific community was devoted to devising suitable models to properly account for the setting of the SF behavior. The main streams in this research have mostly pursued two principal lines: a statistical approach and an adaptive approach. As for the statistical models, they can be classified into two main classes: the nongrowing models, and the growing models. The former class includes those models that, starting from the entire set of nodes, establish specific linking rules that produce the desired degree distribution while the latter class includes those models for which the degree distribution is the result of a process through which an initial network grows in time by acquiring new nodes (or links), with proper statistical rules for attaching the added nodes (or setting the new links) to those of the pristine graph.

The most famous nongrowing model is the so-called *configuration model*, which was introduced by Bender and Can-

field [3], with the aim of constructing a random graph displaying an arbitrary degree distribution. As for the class of growing models, one has to refer to the original Barabási-Albert model of preferential attachment [4] to its many extensions, as well as to alternative models that do not explicitly make use of preferential attachment rules, such as those arising from the so-called vertex copying and duplication mechanisms [5].

On the other side, regarding the adaptive approach, it has to be mentioned that SF configurations have been obtained either by considering an evolutionary preferential attachment process on top of a network growth ruled by an adaptive capacity of nodes to attract links depending on the dynamical state of the network [6], or as a consequence of network functioning readjustment due to successive node deletion and correspondent preferential redistribution of the deleted node quality (fitness) among its neighbors [7]. A recent review [8] summarizes the most important results on adaptive (evolutionary) processes, and their influence into reshaping and/or selecting the structural form of a network.

In more recent years, the attention has concentrated to understanding the intimate relationship between the topological structure displayed by a graph, and the mechanisms leading to the arousal of a collective behavior (as, e.g., the synchronization of all the network's nodes into a common dynamical behavior) [2,9,10]. Recent studies have, indeed, shown that (i) the ability of a graph to give rise to a synchronous behavior can be greatly enhanced by exploiting the topological structure emerging from independent statistically driven growth processes [11]; (ii) proper topological mechanisms of rewiring and decoupling can enhance the arousal of a synchronized behavior [12]; (iii) a dynamical evolution of the underlying topology of a graph is eventually able to stabilize a synchronous motion also in those cases in which synchronization would be prevented in static graph configurations [13].

In particular, the discussion on the relationship between network's structure and dynamics started with the observation that synchrony can be even deteriorated when increasing

the heterogeneity in the connectivity distribution of a un-weighted network at the same average network distance [14], and later advanced with the evidence that such a limitation could be properly overcome by a suitable weighting procedure [2,11].

However, a full understanding on how graph functioning can be responsible alone for the arousal of a given network structure is still an open question. In this paper, we provide the general description of the emergence of scale-free distributions in the network's connectivity in connection with the forcing of a collective (synchronized) network's dynamics of interacting dynamical systems, this way extending the investigation recently reported by us in Ref. [15], and, at the same time, giving full details on the generality and robustness of this relationship between network function and structure.

The paper is organized as follows. In Sec. II we introduce and discuss a model describing a network of bidirectionally coupled phase oscillators subjected to a forcing process from external pacemakers. In Sec. III we present the results of these interacting networks at both the level of the emerging synchronized dynamics, and at the level of the evolution of the underneath topological structure. The understanding of the phenomenon is given in Sec. IV, as well as a detailed analysis of its robustness and reproducibility under different scenarios, such as the presence of noise, alternative coupling functions, or different initial graph configurations. Finally, in Sec. V we summarize some conclusions and give further outlook.

II. MODEL

In this section we start by explaining the details of the model in two steps: first, we introduce the pristine network $\mathcal{G}_0$ (i.e., previous to forcing), as well as some useful parameters to characterize the dynamical state of the network. Next, we describe how the topological structure of the pristine network can be reshaped by means of a forcing process ruled by the dynamics.

A. Pristine network

We consider an initial graph $\mathcal{G}_0$ of N bidirectionally coupled Kuramoto phase oscillators [16]. The equation describing the evolution of the instantaneous phases $\phi_i(t)(i = 1, \ldots, N)$ of the oscillators is

$$\dot{\phi}_i = \omega_{0i} + \frac{d}{k_{0i}} \sum_{j=1}^{N} a_{ij} \sin(\phi_j - \phi_i), \qquad (1)$$

where dot denotes temporal derivative, $\{\omega_{0i}\}$ is the set of natural frequencies of the phase oscillators (randomly taken from a uniform distribution of mean 0.5 and width Δw), $k_{0i} = k_i(t=0)$ is the initial inner degree of the ith oscillator, d is the strength of the bidirectional coupling, and $\mathbf{A} = (a_{ij})$ is the $N \times N$ adjacency matrix of $\mathcal{G}_0$. Time integration is here performed by means of the Heun method with an integration step $\Delta t_{in} = 0.1$ time units (t.u.). Initial conditions for the phases of the oscillators are randomly taken from a uniform distribution in the interval $(0, 2\pi)$.

It is well known that the generic behavior of system (1) displays a transition to phase synchronization at a critical value d_c of the coupling strength [16–18]. All throughout the present work, we will be referring to different graph configurations for $\mathcal{G}_0$, ranging from a simple ring with each node connected to its $k_{0i} = 4$ neighbors to *small-world* graph topologies constructed either by randomly rewiring each link (SW-rew) of the ring with probability $p_{rew} = \log N/N$ (i.e., following the procedure originally introduced by Watts and Strogatz [19]) or just randomly adding a new link (SW-add) per node with the same probability $p_{add} = p_{rew}$, to even SF networks built following the Barabási-Albert model [4] ($m_0^{BA} = 2$ and $m^{BA} = 2$).

In order to properly quantify the degree of synchronization in $\mathcal{G}_0$, we monitor the time evolution of the average frequency in the ensemble

$$\omega(t) = \frac{1}{N} \sum_{i=1}^{N} \dot{\phi}_i,$$

its corresponding standard deviation,

$$\sigma_\omega(t) = \sqrt{\frac{1}{N} \sum_{i=1}^{N} [\dot{\phi}_i - \omega(t)]^2},$$

and the phase synchronization order parameter [16],

$$R(t) = \frac{1}{N} \left| \sum_{j=1}^{N} e^{i\phi_j(t)} \right|,$$

bounded between zero and one (with $R = 1$ if all oscillators are phase synchronized).

The time averages of these quantities in the asymptotic state, $\sigma_\omega = \langle \sigma_\omega(t) \rangle_t$ and $R = \langle R(t) \rangle_t$, are reported in Figs. 1(a) and 1(b) as a function of the coupling strength d for different graph configurations for $\mathcal{G}_0$. It appears evident that in both the SF and SW-add graphs there is a transition to a synchronous state, whose onset occurs around $d_c \simeq 0.5$, while for the more homogeneous graphs (the ring and the SW-rew) only frequency synchronization ($\sigma_\omega \to 0$) is achieved within the range of displayed coupling strengths. As illustrative examples, Figs. 1(c) and 1(d) show the time evolution (vertical axis) of the cosine of the phase of the $N = 100$ oscillators (horizontal axis) arranged in a SF network for two different values of the coupling strength, i.e., below [$d = 0.2$, Fig. 1(c)] and above [$d = 1.0$, Fig. 1(d)] the threshold of the synchronization onset.

In the following we will first restrict our attention to an initial network $\mathcal{G}_0$ with a SW-rew topology and fully desynchronized. Only in Sec. IV we will explore the effect of considering alternative initial topologies.

B. Forcing network

Our aim is to entrain the pristine network $\mathcal{G}_0$, which displays an unsynchronized motion such as the one shown in Fig. 1(c), to a collective motion driven by an external pacemaker of frequency ω_p.

To this purpose, at time $t_0 = 30$ t.u., a forcing network is grown on top of the evolution of $\mathcal{G}_0$. Precisely, at regular
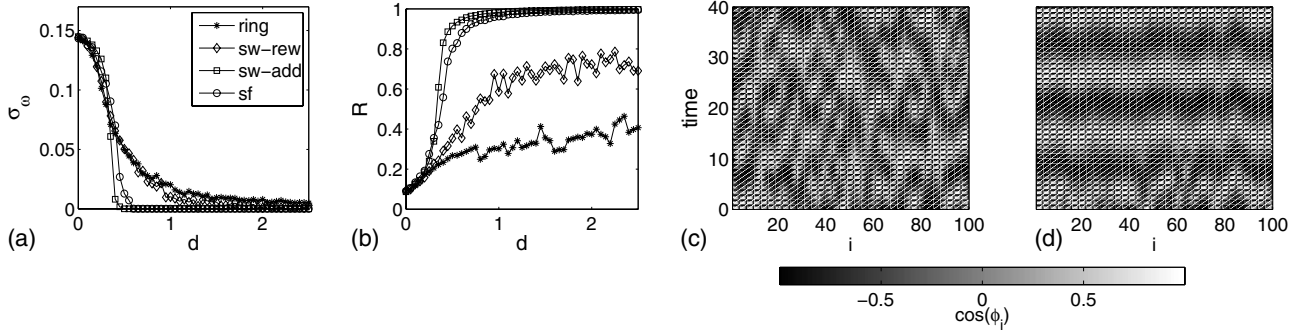
FIG. 1. Synchronization of $\mathcal{G}_0$ before forcing, with $N=100$ nodes, and initial frequencies randomly distributed in the range 0.5 ± 0.25 for different graph configurations (see text for details). Upper row: (a) frequency dispersion σ_ω and (b) phase synchronization order parameter R as functions of the coupling strength d for a ring with $k_i = 4 \, \forall \, i (*)$, a SW with a link rewiring probability of $p_{\text{rew}} = 0.046$ ($\diamond$), a SW with a link adding probability of $p_{\text{add}} = 0.046$ ($\square$), and a SF network ($\bigcirc$). Each reported value of σ_ω and R is the result of an ensemble average over ten network realizations. Lower row: raster plots of the cosine of the phases in a SF coupling configuration for two different coupling strengths, (c) $d=0.2$ and (d) $d=1.0$.

times $t_n = t_0 + n T_{\text{att}}$, we add up to N_p external nodes, (with $n = 1, \ldots, N_p$ and T_{att} as the attaching period), whose phase obeys $\dot{\phi}_p = \omega_p$. Each time a new node is added, it forms m unidirectional connections (of strength d_p) to nodes in $\mathcal{G}_0$.

While, for the sake of illustration, in the following we set $m=1$, the reported scenario is independent on the specific choice of m, the only difference being that, for $m=1$, the added nodes do not form additional cycles nor loops in the original graph $\mathcal{G}_0$.

A sketch of this process is shown in Fig. 2. There, nodes in the pristine network $\mathcal{G}_0$ for $t<t_0$ [Fig. 2(a)] are evolving under the only influence of other nodes of $\mathcal{G}_0$ (dots and links in black), while for $t=t_3 > t_0$ [Fig. 2(b)], the network includes three nodes (in blue) which are unidirectionally coupled (blue thick links) to nodes in $\mathcal{G}_0$. As a consequence, the in-degree $k_i(t)$ of every node in $\mathcal{G}_0$ is an increasing function of time.

The criterion for the evolution of $k_i(t)$ is the key point in the growth of the forcing network. The selection mechanism through which the added nodes are linked to $\mathcal{G}_0$ can be visualized in Figs. 2(c) and 2(d), and it is entirely dependent on the phase state of the network $\mathcal{G}_0$. In Fig. 2(c), the phase difference $\Delta\theta_j(t_n) = \phi_j(t_n) - \phi_p(t_n)$ between the phases of each node in $\mathcal{G}_0$ and that of the pacemaker is represented in the unit circle as a point. These points will rotate in time around the circle, clockwise or counterclockwise depending on whether the difference between the node instantaneous frequency and that of the pacemaker is positive or negative. At time t_n the nth forcing node is added and it selects that node in $\mathcal{G}_0$ whose phase difference $\Delta\theta_j(t_n)$ holds more closely a given phase condition δ. This phase relationship condition is represented as a red line in Fig. 2(d). The node that, at t_3, is the candidate to receive a connection from the $n=3$ forcing pacemaker is the node $i=5$, which therefore will increase its degree from three to four.

More rigorously, we consider a generic parameter $\delta \in (0, 2\pi)$ and establish the connection with that node j_n whose actual value of the phase holds the condition

$$\min_{j=1,\ldots,N} \left| \delta - \Delta\theta_j \bmod 2\pi \right|, \tag{2}$$

with $\Delta\theta_j = \phi_j(t_n) - \phi_p(t_n)$. When $m>1$, we iteratively repeat the same condition excluding those nodes that already received a link at the same time step.

As for the parameter δ, we will show in Sec. IV that it will not affect qualitatively the reported scenario. The only constrain is that it cannot be taken equal to 0 nor to 2π, as
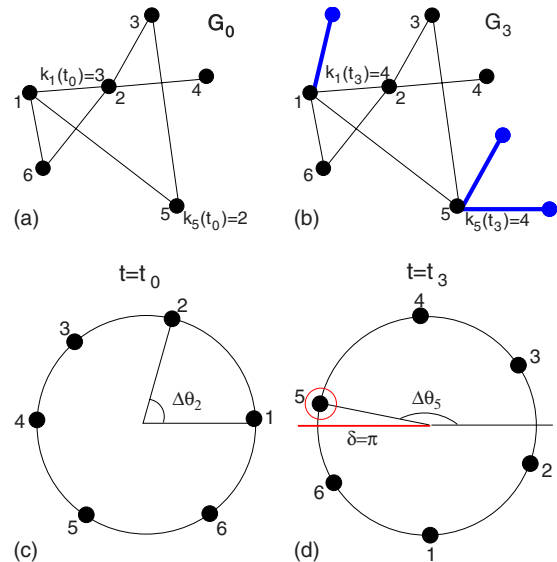

FIG. 2. (Color online) Growth and attaching mechanisms of the forcing process for $m=1$. Upper row: cartoons of the network $\mathcal{G}_0$ in its pristine state [(a) at t_0], and (b) at time t_3 with the corresponding added forcing nodes [$n_p(t_3)=3$] marked in blue. Black thin (blue thick) links are of strength $d(d_p)$, and black (blue) dots oscillate with frequencies within $0.5 \pm \Delta\omega(\omega_p)$. Lower row: representation in the unit circle of the phase differences $\Delta\theta_j(t)$ of each node in $\mathcal{G}_0$ with respect to that of the pacemaker. The red line marks the phase relationship (in this case $\delta=\pi$) and helps to visualize how the phase condition determines the selection of the nodes that receive attachments from the pacemakers (in this case $i=5$ at time t_3).
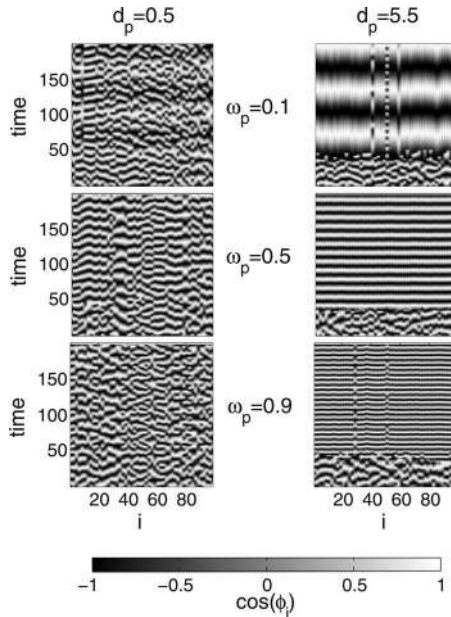
FIG. 3. Raster plots of the cosine of the phases of the oscillators belonging to $\mathcal{G}_0$ for two different coupling regimes, d_p=0.2 (left column) and d_p=5.5 (right column), and for three pacemaker frequencies. Other parameters specified in the text.

these values correspond to the stable fixed point emerging during the entrainment of a single phase oscillator, and therefore these settings would determine a situation in which the first node in $\mathcal{G}_0$ becoming entrained with the pacemaker, would, from there on, attract all the rest of connections.

The network-phase equation is therefore described by

$$\dot{\phi}_i = \omega_{0i} + \frac{d}{k_i(t)}\sum_{j=1}^{N} a_{ij}\sin(\phi_j - \phi_i)$$

$$+ \frac{d_p}{k_i(t)}\sum_{j=1}^{n_p(t)} b_{ij}\sin(\phi_p - \phi_i), \qquad (3)$$

where $k_i(t)$ is the time evolving degree of the ith node that accounts for new connections the ith node is receiving from added nodes following the dynamical criterion given by Eq. (2), and the matrix $\mathbf{B}=(b_{ij})$ is a size evolving matrix of $N \times n_p(t)$ elements [with $n_p(t) \le N_p$], whose entries b_{ij} are equal to one if the jth added node formed a connection with the ith node in $\mathcal{G}_0$, and zero otherwise.

III. RESULTS

The effect of the described forcing network on the entrainment of a small graph $\mathcal{G}_0$ of N=100 oscillators is visible in Fig. 3, which shows the raster plots of the cosine of the oscillators' phases in two regimes of the coupling strength d_p and for three distinct pacemaker frequencies (ω_p=0.1, 0.5, and 0.9). In the low coupling regime (left column), the forcing network (that is composed here by N_p=200 pacemakers) is not able to entrain $\mathcal{G}_0$ to any of the three frequencies, and the raster plots exhibit a disordered behavior. On the other hand, in the high coupling regime (right column), the forcing
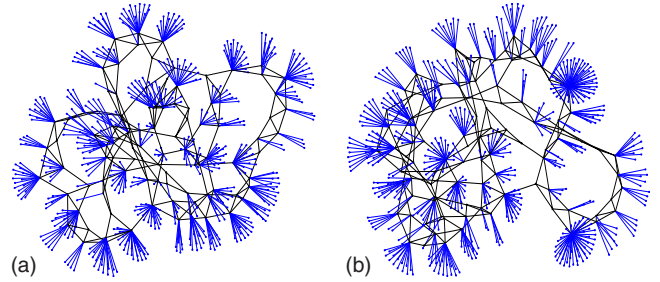

FIG. 4. (Color online) Representation of two networks constructed for N=100, N_p=1000, and $\delta=\pi$. The nodes and links of the original graph are depicted in black while the forcing nodes and links are depicted in blue. The (a) [(b)] network corresponds to a case in which the forcing nodes are unable [able] to eventually lock the phases of the oscillators in.

network eventually controls $\mathcal{G}_0$ and imposes a global oscillation at the prescribed pace, which emerges before the addition of pacemakers stops (t=50 t.u.).

A statistical behavior of the complete dynamical response of $\mathcal{G}_0$ in the d_p-ω_p parameter space is reported in [15]. There it is shown that the forcing network is able to impose its pace in a wide range of the parameter space but it exists as a kind of threshold phenomenon in d_p, whose critical value for the entrainment depends on the pacemaker frequency. Specifically, as far as ω_p is close to the mean value of the set of natural frequencies in $\mathcal{G}_0(0.5)$, the frequency and phase entrainment process occurs already for a relatively small value of d_p, whereas, as ω_p deviates significantly from 0.5, the value of d_p that produces phase entrainment becomes larger and larger.

Our main goal is to inspect the changes in the network topology induced by the entrainment process. The way the forcing process couples dynamics and topology makes that, indeed, some nontrivial features in the structure emerge from this interplay. In particular, the final degree distribution associated to the entrainment of $\mathcal{G}_0$ becomes heterogeneous if compared to the exponentially decaying distribution characterizing its initial wiring structure. This effect is illustrated in Fig. 4, which reports the graphical representation of two networks resulting from a forcing process (N=100, N_p=1000) with two different outcomes. The left network features a rather homogeneous distribution of the links from the pacemakers to $\mathcal{G}_0$ (blue links), and corresponds to the graph structure associated to an incoherent phase dynamics during the whole evolution of the system (i.e., in a coupling regime that does not induce entrainment). On the contrary, the right plot unveils the presence of few nodes receiving a much larger number of incoming links with respect to the rest of graph. The relevant point is that such a kind of inhomogeneous distributions are *always* related to cases for which an entrainment of $\mathcal{G}_0$ is achieved (i.e., for sufficiently large values of the coupling strength d_p).

To properly quantify the emergence of this heterogeneity in the degree distribution, we perform large trials of numerical simulations with N=1000, N_p=10 000, and d=0.2, and we monitor the time evolution of the degree distribution $P_t(k)$ of all nodes originally belonging to $\mathcal{G}_0$ during the process of forcing.
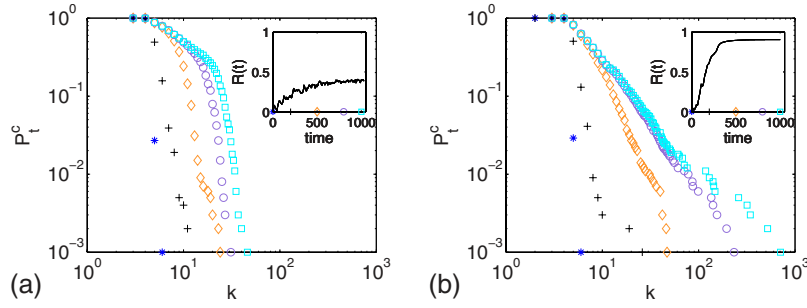
FIG. 5. (Color online) Time evolution of the cumulative degree distribution $P^c(k)$ in a double-logarithmic plot for a specific realization of the growing process with $N=1000$, $N_p=10\,000$, and $d=0.2$. (a) $\omega_p=0.5$ and $d_p=0.2$ (nonentrained graph) and (b) $d_p=0.5$ (entrained graph). In both cases the inset reports the corresponding time evolution of $R(t)$. The time instants at which the distributions are taken (indicated in the time axis of the insets by their corresponding symbol) are: $t=0(*)$; $t=200(+)$; $t=500$ ($\Diamond$); $t=800$ ($\bigcirc$); $t=1000$ ($\Box$). Notice that, in the entrained case, $P_t^c(k)$ converges to an asymptotic distribution ($\Box$) which features a power-law shape.

In fact, we here measure the *cumulative* degree distribution $P_t^c(k)$, given by

$$P_t^c(k) = \sum_{k'=k}^{k_{\max}} P_t(k').$$

This is because the summing process of the $P(k)$ smoothes the statistical fluctuations generally present in the tails of the distribution. As a generic property, it is important to remark that, if a power-law scaling is observed in the behavior of $P^c(k)$ [i.e., if $P^c(k) \sim k^{-\gamma_c}$], this implies that also the degree distribution $P(k)$ is characterized by a power-law scaling $P(k) \sim k^{-\gamma}$, with

$$\gamma = 1 + \gamma_c.$$

Figure 5 reports how $P_t^c(k)$ evolves in time in the two different coupling regimes: when d_p is small enough so that the forcing does not lead to any entrainment [Fig. 5(a)], and for a process that eventually leads to entrainment of $\mathcal{G}_0$ to the frequency of the pacemaker [Fig. 5(b)]. In both cases, the insets report the corresponding evolution of $R(t)$.

One immediately realizes that, in Fig. 5(a), $P_t^c(k)$ does not deviate significantly in shape from its initial distribution $P_0^c(k)$, and the only effect of the forcing network in the degree distribution is to uniformly increase the mean degree. At variance, Fig. 5(b) shows that the entrainment process [manifested by the evolution of $R(t)$ to one in the inset] is accompanied by the convergence of $P_t^c(k)$ to an asymptotic distribution $P_{\mathrm{fin}}^c(k)$ which features a power-law shape.

The difference in the final distributions for the nonentrained and entrained networks, and the convergence in this latter case of $P_t^c(k)$ to a SF distribution $P_{\mathrm{fin}}^c(k)$ is independent of the pacemaker frequency as reported in [15]. The specific slope γ of the power-law scaling does, instead, depend on the specific choice of the external frequency ω_p. In our trials, we always observed values of γ in the range (2,3), in accordance to the values measured for most of the real world networks [1]. In the following we will discuss the details of the mechanism leading to the appearance of a SF degree distribution in connection with a locking of the network's frequencies to the external pacemaker, and we will show that the proposed attachment mechanism there gradually turns

into a preferential attachment process, wherein the larger is the oscillator initial frequency difference with the pacemaker while the higher is its probability of acquiring more and more connections during the growth process.

IV. DISCUSSION

A. Mechanism for the emergence of the scale-free distribution

In order to explain the mechanism behind the emergence of the scale-free degree distribution associated to the entrainment of the network, let us go back to the representation in the unit circle of the state of the network $\mathcal{G}_0$ through the phase differences $\Delta\theta_i(t)$ introduced in Sec. II. In that representation, if a given node in $\mathcal{G}_0$ at some point locks its phase to that of the pacemaker, one would have a corresponding value $\Delta\theta_i \sim 0$, and its phase difference vector will be locked in the unit circle in the vicinity of the state $\Delta\theta=0$. As a consequence, as far as δ is strictly different from 0 and 2π, the node will not be likely to receive any further connection.

Now, when the forcing network is unable to entrain $\mathcal{G}_0$, each node of $\mathcal{G}_0$ will be represented by a point that continuously rotate in the unit circle (clockwise or counterclockwise) with a rotation frequency larger or smaller depending on the actual difference between the frequency of the node and that of the pacemaker. In such a condition, it is easy to realize that the probability of locating the phase vector $\Delta\theta_i$ near the desired phase condition δ [marked with the red line in Fig. 2(d)] will be *independent* on the specific rotation frequency of the representing point: if, indeed, the rotation frequency is higher (lower), the time spent in the vicinity of the phase relationship marker will be smaller (larger) but the rate of crossing the marker will be equally larger (smaller). As a result, the attaching process of the pacemakers is almost equivalent to a random attachment, where at different times, the additional pacemakers will select randomly the node to form an attachment with.

Initially, $\mathcal{G}_0$ is prepared in an incoherent state, and therefore, before the forcing process starts, the phase differences are randomly distributed in the unit circle. As soon as pacemakers are incorporated to the forcing network, if the coupling strength d_p is small enough not to produce locked states (e.g., $d_p=0.2$), almost all the nodes will remain un-
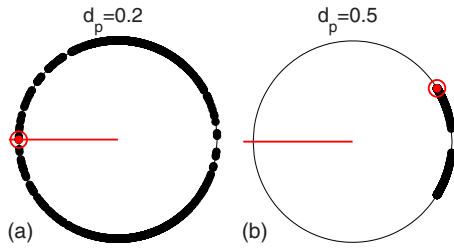
FIG. 6. (Color online) Phase differences $\Delta\theta_j$ of the oscillators with respect to that of the pacemaker distributed along the unit circle at the end of (a) a frustrated locking process ($d_p=0.2$) and (b) a successful locked one ($d_p=0.5$). The red line indicates the phase relationship for the attaching rule $\delta=\pi$, and the red circle indicates the node that is receiving a link from a pacemaker at the time the picture was taken.

FIG. 7. (Color online) Final number of connections $k_i(t_{fin})$ acquired by each node as a function of its initial frequency ω_{0i} for $\omega_p=0.5$, $\delta=\pi$, and $d_p=0.2$ (upper plot, unlocked case) and $d_p=0.5$ (lower plot, locked case).

locked (except maybe those few ones whose original frequency was occasionally sufficiently close to that of the pacemaker). In this case, the representing points will continue rotating in the unit circle, and the attachment process will continue being almost random through the entire network's growth, thus preserving the initial distribution of the phase differences, as shown in Fig. 6(a). On its turn, this implies that, as pacemakers will randomly attach to nodes in $\mathcal{G}_0$, the arising degree distribution will be similar to those characterizing random graphs, i.e., with Gaussian or Poissonian decaying tails, as the one shown in Fig. 5(a).

On the other hand, when the coupling strength d_p is larger, some nodes, especially those whose frequencies are closer to that of the pacemaker, become progressively locked by the forcing network and they are the first ones that will accumulate in the region around $\Delta\theta=0$, as shown in Fig. 6(b). This provokes a progressive increase in the probability of the remaining untrained nodes of receiving a link from the pacemaker since they remain the only ones competing for receiving further attachments.

This mechanism is well illustrated in Fig. 6, which reports snapshots of the dynamical state of the phase differences of the nodes in $\mathcal{G}_0$, at the end of both a frustrated locking process [Fig. 6(a)] and of a successful entrainment [Fig. 6(b)].

The corresponding effect on the resulting topology is reported in Fig. 7, where the final number of connections k_i acquired by each node of $\mathcal{G}_0$ after all forcing pacemakers have been added, is plotted as a function of its natural (initial) frequency ω_{0i}. It is evident that, for a low forcing coupling regime, $d_p=0.2$ (when entrainment fails), the distribution of the final degree is quite homogeneous among the initial distribution of frequencies [Fig. 7(a)], indicating that a kind of a random shooting has taken place during the attachment process. In accordance with the dynamical description given before, in this regime, nodes in $\mathcal{G}_0$ remain unlocked during the whole process, and their probability of being close to the attaching condition (red line in Fig. 6) is independent of their initial frequency.

On the other hand, in the high coupling regime, $d_p=0.5$, while initially the attaching process is at random, as more and more oscillators in $\mathcal{G}_0$ progressively become locked, the process gradually turns into a preferential attachment in frequency difference (it is, indeed, reasonable that the first
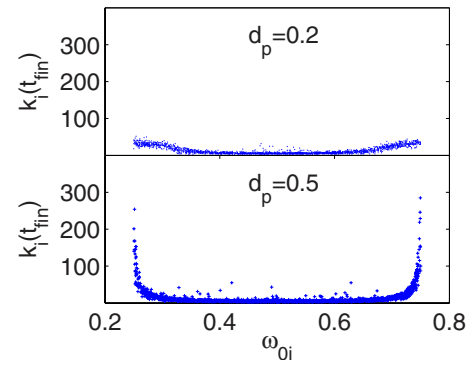
nodes to lock will be the ones whose original frequency was closer to that of the pacemaker). This is reflected by the fact that the final degree distribution peaks around the extremes of the natural frequency distribution [Fig. 7(b)].

B. Robustness of the scale-free emergence

It is relevant to notice that the emergence of a scale-free fingerprint in the degree distribution associated to a global entrainment of the network is a robust feature against variations in the initial conditions, in the attaching parameters, and against fluctuations in the pacemaker oscillations.

In order to test the robustness of this phenomenon, we computed the cumulative degree distribution $P^c(k)$ simulating a series of different scenarios. First, we considered different initial configurations for the initial topology and dynamics. In Fig. 8(a) we observe that, regardless on the chosen pristine architecture for $\mathcal{G}_0$ [the different initial distributions $P^c(t=0)$ are plotted in the inset of the panel], the stationary cumulative degree distribution approaches a straight line in a double-logarithmic scale. In all these cases, the oscillatory network achieves a synchronous state entrained with the forcing network, and even for the very regular topology, such as the ring configuration (orange squares), the final degree distribution results heterogeneous.

Figure 8(b) accounts, instead, for the robustness of the process against variations in the initial dynamical conditions for $\mathcal{G}_0$. In particular, we observe that the results are not qualitatively changing by varying the width of the uniform distribution of natural frequencies in $\mathcal{G}_0$. An interesting point is that, without loosing the power-law scaling feature, it can be seen that the more heterogeneous is the oscillator population, the lower is the maximum degree. This can be easily understood if one takes into account that in all cases, the size of the forcing network is the same while it is reasonable that the case of highest disorder would require a larger number of pacemakers in order to achieve entrainment. In fact, the average value of the Kuramoto parameter for $\Delta\omega=0.50$ (the only plotted case for which the entrainment is not achieved) is not even close to 1.0 ($R=0.48$).

Another important dynamical aspect ruling the behavior of the network is the specific nature of the coupling function,
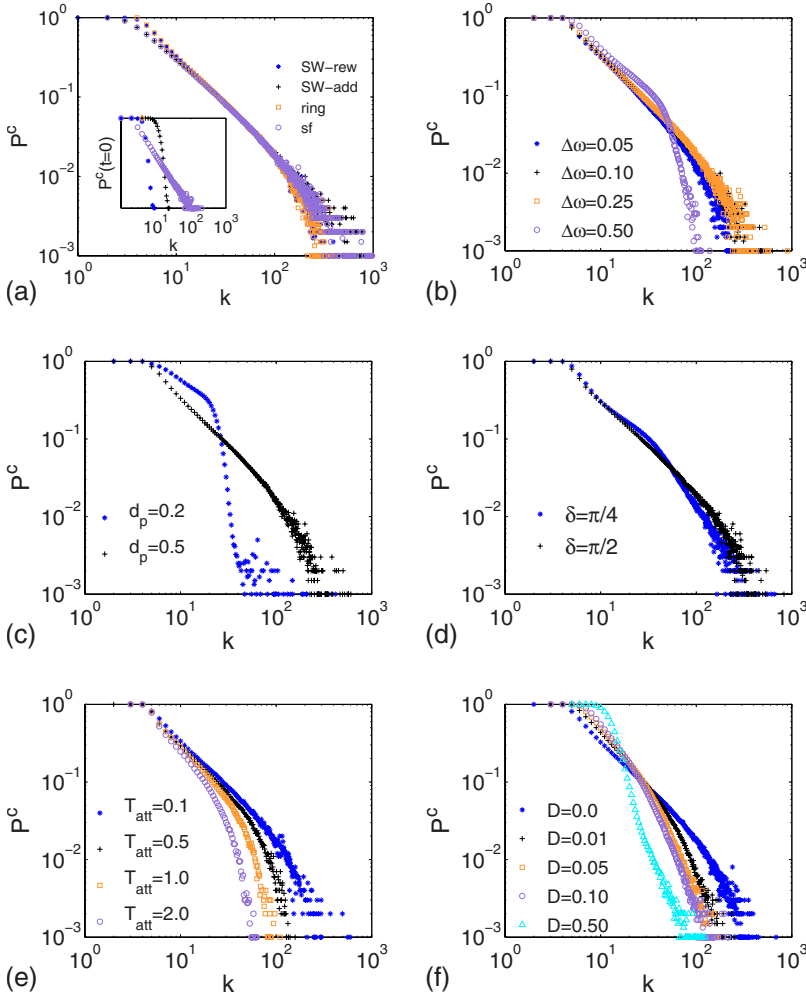
FIG. 8. (Color online) Robustness of the power-law shape behavior of the stationary cumulative degree distribution P_c (double-logarithmic plots) under different cases. (a) Different initial degree distributions for the pristine network, SW with rewiring probability p_{rew} =0.0069, SW with adding probability p_{add} =0.0069, a ring configuration with four nearest neighbors, and a SF network; (b) different natural frequency dispersions $\Delta\omega$=0.05, 0.10, 0.25, 0.5; (c) a coupling term in Eq. (3) containing the sum of the third power of the sinus of phase differences; (d) different values of the phase relationship δ [δ=π/4 and π/2], for the attachment rule; (e) different attaching periods T_{att}=0.1, 0.5, 1.0, and 2.0 t.u.; (f) different levels of white-noise intensities (D=0.5, 0.1, 0.05, 0.01, and D=0) affecting the evolution of the pacemaker. In all cases, unless differently indicated in the corresponding panel: N=1000, N_p=10 000, d=0.2, d_p=0.5, δ=π, SW-rew with p_{rew}=0.0069 as initial topology for the graph, $\Delta\omega$=0.25, and T_{att} =0.1 t.u.

that is, the function that transfers the state from one oscillator to its neighbors. Therefore, it is important to show that the process reported so far is not dependent on the specific Kuramoto model equation that is implemented on the network's nodes. If, indeed, we repeat the same numerical trials by substituting the coupling term of Eq. (3) with

$$\frac{d}{k_i(t)}\sum_{j=1}^{N} a_{ij} \sin^3(\phi_j - \phi_i) + \frac{d_p}{k_i(t)}\sum_{j=1}^{n_p(t)} b_{ij} \sin^3(\phi_p - \phi_i),$$

we obtain the same qualitative scenario, in which the eventual phase entrainment of the oscillators in $\mathcal{G}_0$ is always associated with the appearance of a scale-free distribution in the final graph connectivity.

Figures 8(d) and 8(e) deal with the dependence of the observed scenario on the parameters defining the attaching mechanism, that is, the phase condition δ [Fig. 8(d)], and the attaching period T_{att}, [Fig. 8(e)]. In Sec. II, we already discussed the admissible values for δ, especially the fact that δ must be strictly different from 0 and 2π. We investigated the effect of this parameter on the shape of $P^c(k)$ assuming two values, δ=π/2 and δ=π/4, different from the optimal one, δ=π, which more effectively induces an entrainment in $\mathcal{G}_0$.

The results are shown in Fig. 8(d), and again depict a similar qualitative behavior as that reported for δ=π. Only

for δ=π/4 (blue stars), which is a close value to the forbidden phase relationship, a small bump for medium degrees appears, distorting a little bit the power-law trend. As for the period of attaching a new pacemaker to $\mathcal{G}_0$, we observe that the power-law behavior is preserved with variations in T_{att}. The only difference is the size of the degree interval where it holds which decreases as T_{att} increases. This is due to the fact that a given pacemaker has more time to control part of the network before the addition of a new one, giving rise to a minor number of needed pacemakers to entrain the whole network.

The last panel of Fig. 8 reports the results of simulations aimed to test the robustness of the emergence of the scale-free in $\mathcal{G}_0$ in the presence of fluctuations in the pacemakers, that is, by considering that the phase evolution of the forcing network is affected by some white noise of zero mean and intensity D, $\dot{\phi}_p = \omega_p + \xi(t)$, where $\langle \xi(t), \xi(t') \rangle = 2D\delta(t-t')$. The power-law behavior is clearly lost for very large noise intensities (D=0.5) which is accompanied with a lost in the level of entrainment (σ_ω=0.2 and R=0.73) but for small noise intensity values, the fluctuating forcing network is still able to entrain $\mathcal{G}_0$, and again the way the entrainment is achieved is associated with the appearance of a SF degree distribution for the nodes of $\mathcal{G}_0$.

Finally, we point out that no qualitative differences are observed in the described scenario for different values of the

internal coupling strength d, provided that it is kept below the threshold for the synchronization onset of the initial graph $\mathcal{G}_0$.

V. CONCLUSIONS

In conclusion, we have shown that the topology and dynamics of a network of phase oscillators can be controlled at once by means of a forcing mechanism which entrains the phases of the oscillators to that of an external pacemaker in connection with the reshaping of the network degree distribution. We have furthermore proven that a dynamically based rule in the attachment process leads to the emergence of a power-law shape in the final degree distribution in the original graph whenever the network is entrained to the dynamics of the pacemaker, and that the arousal of a scale-free distribution in connection with the success of the entrainment process is a robust feature, characterizing different network's initial configurations and parameters.

While several other studies have pointed out that networks' topology and functioning are intimately and not trivially related (and, actually, SF topologies can optimize collective synchronous behavior if associated to a proper weighting procedure [2,11] or to an adaptive graph evolution [6,7]), here we demonstrate that power-law tails in the connectivity distribution (and hence the emergence of hubs and degree heterogeneity) can be a direct consequence of a controlled entrainment onto a generic initial topology of networking continuous time dynamical systems.

In particular, the most relevant aspect of our approach consists in the fact that a merely dynamical rule [Eq. (2)] can encompass at once a preferential-like attachment procedure (when a collective state is promoted) and a sort of random-like attachment giving rise to a homogeneous connectivity distribution (when synchronization is not established).

The evidence that a purely dynamical mechanism can induce the emergence of specific power-law degree distributions can provide new insights on the fundamental processes at the basis of the growth of some of the real world networks, which seem to, indeed, feature ubiquitously such kind of connectivity distributions.

ACKNOWLEDGMENTS

[1] R. Albert and A. L. Barabási, Rev. Mod. Phys. **74**, 47 (2002); M. E. J. Newman, SIAM Rev. **45**, 167 (2003).

[2] S. Boccaletti, V. Latora, Y. Moreno, M. Chavez, and D.-U. Hwant, Phys. Rep. **424**, 175 (2006).

[3] E. A. Bender and E. R. Canfield, J. Comb. Theory, Ser. A **24**, 296 (1978).

[4] A. L. Barabási and R. Albert, Science **286**, 509 (1999).

[5] J. M. Kleinberg, R. Kumar, P. Raghavan, S. Rajagopalan, and A. Tomkins, Lect. Notes Comput. Sci. **1627**, 1 (1999); J. Kim, P. L. Krapivsky, B. Kahng, and S. Redner, Phys. Rev. E **66**, 055101(R) (2002); F. Chung, L. Lu, T. G. Dewey, and D. J. Galas, J. Comput. Biol. **10**, 677 (2003); A. Vazquez, A. Flammini, A. Maritan, and A. Vespignani, ComPlexUs **1**, 38 (2003); S. Boccaletti, D.-U. Hwang, and V. Latora, Int. J. Bifurcation Chaos Appl. Sci. Eng. **17**, 2447 (2007).

[6] J. Poncela, J. Gómez-Gardeñes, L. M. Floria, A. Sánchez, and Y. Moreno, PLoS ONE **3**, e2449 (2008).

[7] H. Ohtsuki, C. Hauert, E. Lieberman, and M. A. Nowak, Nature (London) **441**, 502 (2006).

[8] T. Gross and B. Blasius, J. R. Soc., Interface **5**, 259 (2008).

[9] F. Sorrentino and E. Ott, Phys. Rev. Lett. **100**, 114101 (2008).

[10] T. Nishikawa and A. E. Motter, Phys. Rev. E **73**, 065106(R) (2006).

[11] A. E. Motter, C. Zhou, and J. Kurths, Phys. Rev. E **71**, 016116 (2005); M. Chavez, D. U. Hwang, A. Amann, H. G. E. Hentschel, and S. Boccaletti, Phys. Rev. Lett. **94**, 218701 (2005); D. U. Hwang, M. Chavez, A. Amann, and S. Boccaletti, *ibid.* **94**, 138701 (2005).

[12] C.-Y. Yin, W.-X. Wang, G. Chen, and B.-H. Wang, Phys. Rev. E **74**, 047102 (2006).

[13] I. V. Belykh, V. N. Belykh, and M. Hasler, Physica D **195**, 188 (2004); D. J. Stilwell, E. M. Bollt, and D. G. Roberson, SIAM J. Appl. Dyn. Syst. **5**, 140 (2006); S. Boccaletti, D. U. Hwang, M. Chavez, A. Amann, J. Kurths, and L. M. Pecora, Phys. Rev. E **74**, 016102 (2006).

[14] T. Nishikawa, A. E. Motter, Y. C. Lai, and F. C. Hoppensteadt, Phys. Rev. Lett. **91**, 014101 (2003).

[15] I. Sendiña-Nadal, J. M. Buldú, I. Leyva, and S. Boccaletti, PLoS ONE **3**, e2644 (2008).

[16] Y. Kuramoto, *Chemical Oscillations, Waves, and Turbulence* (Springer, Berlin, 1984).

[17] S. H. Strogatz, Physica D **143**, 1 (2000).

[18] Y. Moreno and A. F. Pacheco, Europhys. Lett. **68**, 603 (2004).

[19] D. J. Watts and S. H. Strogatz, Nature (London) **393**, 440 (1998).